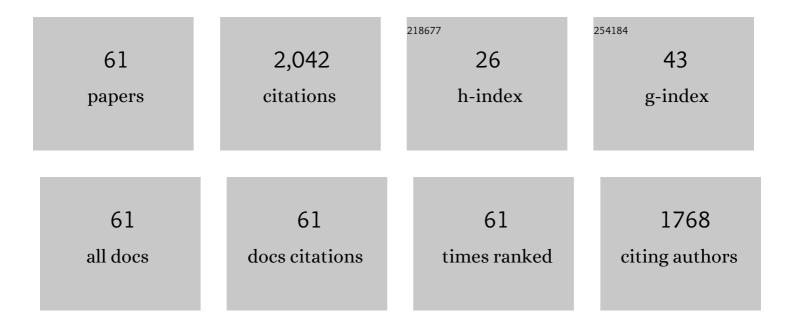
Giovanni B Andreozzi

List of Publications by Year in descending order

Source: https://exaly.com/author-pdf/525379/publications.pdf Version: 2024-02-01



#	Article	IF	CITATIONS
1	Raman fingerprint of chromate, aluminate and ferrite spinels. Journal of Raman Spectroscopy, 2015, 46, 1255-1264.	2.5	280
2	Cation ordering and structural variations with temperature in MgAl ₂ O ₄ spinel: An X-ray single-crystal study. American Mineralogist, 2000, 85, 1164-1171.	1.9	137
3	Influence of cation distribution on the optical absorption spectra of Fe 3+ -bearing spinel s.s. -hercynite crystals: evidence for electron transitions in VI Fe 2+ - VI Fe 3+ clusters. Physics and Chemistry of Minerals, 2002, 29, 319-330.	0.8	59
4	Crystal chemistry of the elbaite-schorl series. American Mineralogist, 2005, 90, 1784-1792.	1.9	59
5	Linking Mossbauer and structural parameters in elbaite-schorl-dravite tourmalines. American Mineralogist, 2008, 93, 658-666.	1.9	54
6	Ni-free, black ceramic pigments based on Co—Cr—Fe—Mn spinels: A reappraisal of crystal structure, colour and technological behaviour. Ceramics International, 2013, 39, 9533-9547.	4.8	54
7	Structural relaxation around Cr3+ and the red-green color change in the spinel (sensu) Tj ETQq1 1 0.784314 rgBT solid-solution series. American Mineralogist, 2010, 95, 456-462.	/Overlock 1.9	10 Tf 50 50 53
8	Combined use of X-ray photoelectron and Mössbauer spectroscopic techniques in the analytical characterization of iron oxidation state in amphibole asbestos. Analytical and Bioanalytical Chemistry, 2010, 396, 2889-2898.	3.7	50
9	A Mössbauer and structural investigation of Fe-ZSM-5 catalysts: Influence of Fe oxide nanoparticles size on the catalytic behaviour for the NO-SCR by C3H8. Applied Catalysis B: Environmental, 2011, 102, 215-223.	20.2	50
10	Crystal structure and iron topochemistry of erionite-K from Rome, Oregon, U.S.A American Mineralogist, 2009, 94, 1262-1270.	1.9	49
11	Kinetics of cation ordering in synthetic MgAl ₂ O ₄ spinel. American Mineralogist, 2002, 87, 838-844.	1.9	46
12	Behavior of cation vacancy in kenotetrahedral Cr-spinels from Albanian eastern belt ophiolites. American Mineralogist, 2004, 89, 1367-1373.	1.9	45
13	The chemical environment of iron in mineral fibres. A combined X-ray absorption and Mössbauer spectroscopic study. Journal of Hazardous Materials, 2015, 298, 282-293.	12.4	44
14	Fe2+ and Fe3+ quantification by different approaches and fO2 estimation for Albanian Cr-spinels. American Mineralogist, 2006, 91, 907-916.	1.9	43
15	Structural refinement and crystal chemistry of Mn-doped spinel: A case for tetrahedrally coordinated Mn3+ in an oxygen-based structure. American Mineralogist, 2007, 92, 27-33.	1.9	42
16	N2O decomposition over [Fe]-MFI catalysts: Influence of the Fe O nuclearity and the presence of framework aluminum on the catalytic activity. Journal of Catalysis, 2014, 318, 1-13.	6.2	40
17	Intersite distribution of Fe ²⁺ and Mg in the spinel (sensu stricto)–hercynite series by single-crystal X-ray diffraction. American Mineralogist, 2002, 87, 1113-1120.	1.9	39
18	Spectroscopic active IV Fe 3+ - VI Fe 3+ clusters in spinel-magnesioferrite solid solution crystals: a potential monitor for ordering in oxide spinels. Physics and Chemistry of Minerals, 2001, 28, 435-444.	0.8	36

#	Article	IF	CITATIONS
19	Blue spinel crystals in the MgAl2O4-CoAl2O4 series: Part II. Cation ordering over short-range and long-range scales. American Mineralogist, 2012, 97, 1834-1840.	1.9	35
20	Compositional dependence of cation distribution in some synthetic (Mg,Zn)(Al,Fe3+)2O4 spinels. European Journal of Mineralogy, 2001, 13, 391-402.	1.3	33
21	Experimental evidence for partial Fe ²⁺ disorder at the <i>Y</i> and <i>Z</i> sites of tourmaline: a combined EMP, SREF, MS, IR and OAS study of schorl. Mineralogical Magazine, 2015, 79, 515-528.	1.4	31
22	Spectroscopic study of the product of thermal transformation of chrysotile-asbestos containing materials (ACM). European Journal of Mineralogy, 2010, 22, 535-546.	1.3	30
23	Iron from a geochemical viewpoint. Understanding toxicity/pathogenicity mechanisms in iron-bearing minerals with a special attention to mineral fibers. Free Radical Biology and Medicine, 2019, 133, 21-37.	2.9	30
24	Fe–Zn manganite spinels and their carbonate precursors: preparation, characterization and catalytic activity. Applied Catalysis B: Environmental, 2005, 57, 153-165.	20.2	28
25	Crystallographic and spectroscopic characterization of a natural Zn-rich spinel approaching the endmember gahnite (ZnAl ₂ O ₄) composition. Mineralogical Magazine, 2013, 77, 2941-2953.	1.4	28
26	The elasticity of MgAl2O4-MnAl2O4 spinels by Brillouin scattering and an empirical approach for bulk modulus prediction. American Mineralogist, 2015, 100, 644-651.	1.9	28
27	Zn-O tetrahedral bond length variations in normal spinel oxides. American Mineralogist, 2011, 96, 594-598.	1.9	27
28	Surface reactivity of amphibole asbestos: a comparison between crocidolite and tremolite. Scientific Reports, 2017, 7, 14696.	3.3	27
29	Short-range order of Fe2+ in sphalerite by 57Fe Mössbauer spectroscopy and magnetic susceptibility. Physics and Chemistry of Minerals, 2005, 32, 339-348.	0.8	26
30	Redox state of subcontinental lithospheric mantle and relationships with metasomatism: insights from spinel peridotites from northern Victoria Land (Antarctica). Contributions To Mineralogy and Petrology, 2012, 164, 1053-1067.	3.1	26
31	Thermodynamics and kinetics of cation ordering in natural and synthetic Mg(Al,Fe3+)2O4 spinels from in situ high-temperature X-ray diffraction. American Mineralogist, 2006, 91, 306-312.	1.9	25
32	Geothermometric study of Cr-spinels of peridotite mantle xenoliths from northern Victoria Land (Antarctica). American Mineralogist, 2014, 99, 839-846.	1.9	25
33	Color mechanisms in spinel: cobalt and iron interplay for the blue color. Physics and Chemistry of Minerals, 2015, 42, 431-439.	0.8	25
34	STRUCTURAL AND CHEMICAL CONTRASTS BETWEEN PRISMATIC AND FIBROUS FLUORO-EDENITE FROM BIANCAVILLA, SICILY, ITALY. Canadian Mineralogist, 2007, 45, 249-262.	1.0	25
35	Surface alteration mechanism and topochemistry of iron in tremolite asbestos: A step toward understanding the potential hazard of amphibole asbestos. Chemical Geology, 2015, 405, 28-38.	3.3	24
36	Thermal behaviour of chlorite: an in situ single-crystal and powder diffraction study. European Journal of Mineralogy, 2009, 21, 581-589.	1.3	23

#	Article	IF	CITATIONS
37	Detailed crystal chemistry and iron topochemistry of asbestos occurring in its natural setting: A first step to understanding its chemical reactivity. Chemical Geology, 2010, 277, 197-206.	3.3	23
38	Dissolution reaction and surface iron speciation of UICC crocidolite in buffered solution at pH 7.4: A combined ICP-OES, XPS and TEM investigation. Geochimica Et Cosmochimica Acta, 2014, 127, 221-232.	3.9	23
39	Diamond-inclusion system recording old deep lithosphere conditions at Udachnaya (Siberia). Scientific Reports, 2019, 9, 12586.	3.3	23
40	Crystal chemical and structural characterization of fibrous tremolite from Susa Valley, Italy, with comments on potential harmful effects on human health. American Mineralogist, 2008, 93, 1349-1355.	1.9	22
41	Structural and spectroscopic characterization of a suite of fibrous amphiboles with high environmental and health relevance from Biancavilla (Sicily, Italy). American Mineralogist, 2009, 94, 1333-1340.	1.9	21
42	Blue spinel crystals in the MgAl2O4-CoAl2O4 series: Part I. Flux growth and chemical characterization. American Mineralogist, 2012, 97, 1828-1833.	1.9	21
43	Surface chemistry and surface reactivity of fibrous amphiboles that are not regulated as asbestos. Analytical and Bioanalytical Chemistry, 2012, 404, 821-833.	3.7	21
44	57Fe Mössbauer and electronic spectroscopy study on a new synthetic hercynite-based pigment. Journal of the European Ceramic Society, 2004, 24, 821-824.	5.7	19
45	A critical comment on Ertl et al. (2012): "Limitations of Fe2+ and Mn2+ site occupancy in tourmaline: Evidence from Fe2+- and Mn2+-rich tourmaline". American Mineralogist, 2013, 98, 2183-2192.	1.9	19
46	Late magmatic controls on the origin of schorlitic and foititic tourmalines from late-Variscan peraluminous granites of the Arbus pluton (SW Sardinia, Italy): Crystal-chemical study and petrological constraints. Lithos, 2018, 308-309, 395-411.	1.4	19
47	Fluor-elbaite, Na(Li1.5Al1.5)Al6(Si6O18)(BO3)3(OH)3F, a new mineral species of the tourmaline supergroup. American Mineralogist, 2013, 98, 297-303.	1.9	18
48	Pressure-volume equation of state for chromite and magnesiochromite: A single-crystal X-ray diffraction investigation. American Mineralogist, 2014, 99, 1248-1253.	1.9	18
49	Iron topochemistry and surface reactivity of amphibole asbestos: relations with in vitro toxicity. Analytical and Bioanalytical Chemistry, 2012, 402, 871-881.	3.7	17
50	Color mechanisms in spinel: a multi-analytical investigation of natural crystals with a wide range of coloration. Physics and Chemistry of Minerals, 2019, 46, 343-360.	0.8	17
51	Site distribution of Fe ²⁺ and Fe ³⁺ in the axinite mineral group: New crystal-chemical formula. American Mineralogist, 2004, 89, 1763-1771.	1.9	14
52	Optical absorption spectroscopy study of the causes for color variations in natural Fe-bearing gahnite: Insights from iron valency and site distribution data. American Mineralogist, 2014, 99, 2187-2195.	1.9	14
53	Petrogenetic controls on the origin of tourmalinite veins from Mandrolisai igneous massif (central) Tj ETQq1 1 0.	784314 rg 1.4	;BŢ/Overlock
		_	

54 Structural study of magnesioaxinite and its crystal-chemical relations with axinite-group minerals. European Journal of Mineralogy, 2000, 12, 1185-1194.

1.3 9

#	Article	IF	CITATIONS
55	Crystal-chemical behavior of Fe2+ in tourmaline dictated by structural stability: insights from a schorl with formula NaY(Fe2+2Al)Z(Al5Fe2+)(Si6O18)(BO3)3(OH)3(OH,F) from Seagull batholith (Yukon) Tj ETQ)q b. B0.78	34 3 14 rgBT
56	In situ high-temperature behaviour of fluor-elbaite: breakdown conditions and products. Physics and Chemistry of Minerals, 2021, 48, 1.	0.8	8
57	Fe–Mg substitution in aluminate spinels: effects on elastic properties investigated by Brillouin scattering. Physics and Chemistry of Minerals, 2018, 45, 759-772.	0.8	6
58	Celleriite, â~{Mn22+Al)Al6(Si6O18)(BO3)3(OH)3(OH), a new mineral species of the tourmaline supergroup. American Mineralogist, 2022, 107, 31-42.	1.9	6
59	HF2EPR spectroscopy of Fe(III) impurities in a blue hercynite-based pigment. Journal of the European Ceramic Society, 2006, 26, 2301-2305.	5.7	3
60	Phlogopite-pargasite coexistence in an oxygen reduced spinel-peridotite ambient. Scientific Reports, 2021, 11, 11829.	3.3	3
61	Iron release in aqueous environment by fresh volcanic ash from Mount Etna (Italy) and Popocatépetl (Mexico) volcanoes, Environmental Earth Sciences, 2018, 77, 1.	2.7	2